Dispersive calculation of hadronic contributions to $(g-2)_\mu$

Gilberto Colangelo

UNIVERSITÄT BERN

AEC
ALBERT EINSTEIN CENTER
FOR FUNDAMENTAL PHYSICS

LatticeNET 2022 – Benasque, September 15

Outline

Introduction: $(g-2)_\mu$ in the Standard Model

Hadronic Vacuum Polarization contribution to $(g-2)_\mu$
- Data-driven approach
- Lattice approach: BMW result and its consequences

Hadronic light-by-light contribution to $(g-2)_\mu$
- Dispersive approach to the hadronic light-by-light tensor
- Short-distance constraints and axial vectors

Conclusions and Outlook

Outline

Introduction: $(g-2)_\mu$ in the Standard Model

Hadronic Vacuum Polarization contribution to $(g-2)_\mu$
- Data-driven approach
- Lattice approach: BMW result and its consequences

Hadronic light-by-light contribution to $(g-2)_\mu$
- Dispersive approach to the hadronic light-by-light tensor
- Short-distance constraints and axial vectors

Conclusions and Outlook

Present status of $(g-2)_\mu$: experiment vs SM

Before

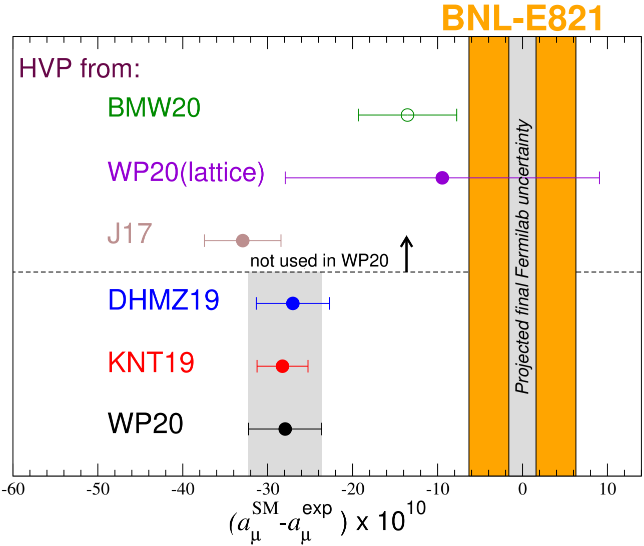

Present status of $(g-2)_\mu$: experiment vs SM

After the Fermilab result

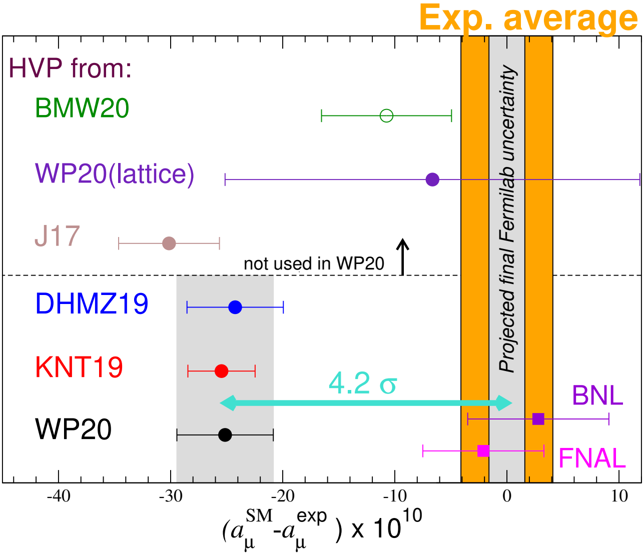

Present status of $(g-2)_\mu$: experiment vs SM

After the Fermilab result

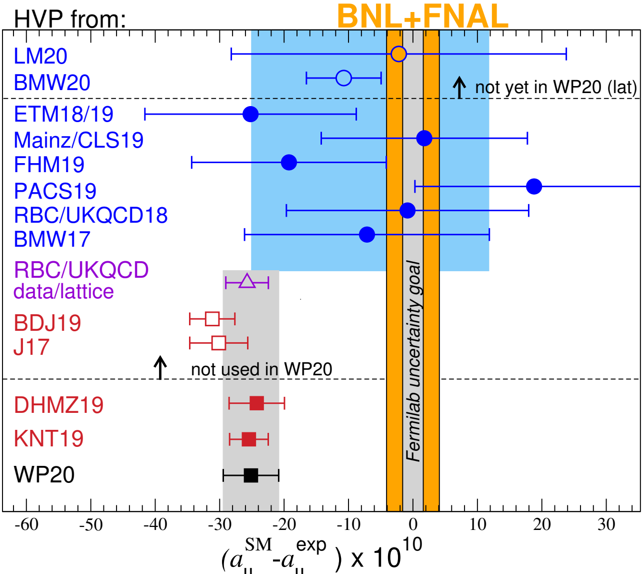

White Paper (2020): $(g-2)_\mu$, experiment vs SM

Contribution	Value $\times 10^{11}$
HVP LO (e^+e^-)	6931(40)
HVP NLO (e^+e^-)	$-98.3(7)$
HVP NNLO (e^+e^-)	12.4(1)
HVP LO (lattice , *udsc*)	7116(184)
HLbL (phenomenology)	92(19)
HLbL NLO (phenomenology)	2(1)
HLbL (lattice, *uds*)	79(35)
HLbL (phenomenology + lattice)	90(17)
QED	116 584 718.931(104)
Electroweak	153.6(1.0)
HVP (e^+e^-, LO + NLO + NNLO)	6845(40)
HLbL (phenomenology + lattice + NLO)	92(18)
Total SM Value	116 591 810(43)
Experiment	116 592 061(41)
Difference: $\Delta a_\mu := a_\mu^{\text{exp}} - a_\mu^{\text{SM}}$	251(59)

White Paper (2020): $(g-2)_\mu$, experiment vs SM

Contribution	Value $\times 10^{11}$
HVP LO (e^+e^-)	6931(40)
HVP NLO (e^+e^-)	$-98.3(7)$
HVP NNLO (e^+e^-)	12.4(1)
HVP LO (lattice BMW(20), *udsc*)	7075(55)
HLbL (phenomenology)	92(19)
HLbL NLO (phenomenology)	2(1)
HLbL (lattice, *uds*)	79(35)
HLbL (phenomenology + lattice)	90(17)
QED	116 584 718.931(104)
Electroweak	153.6(1.0)
HVP (e^+e^-, LO + NLO + NNLO)	6845(40)
HLbL (phenomenology + lattice + NLO)	92(18)
Total SM Value	116 591 810(43)
Experiment	116 592 061(41)
Difference: $\Delta a_\mu := a_\mu^{\text{exp}} - a_\mu^{\text{SM}}$	251(59)

White Paper (2020): $(g-2)_\mu$, experiment vs SM

White Paper:
T. Aoyama et al. Phys. Rep. 887 (2020) = WP(20)

Muon $g-2$ Theory Initiative
Steering Committee:
GC
Michel Davier (vice-chair)
Aida El-Khadra (chair)
Martin Hoferichter
Laurent Lellouch
Christoph Lehner (vice-chair)
Tsutomu Mibe (J-PARC E34 experiment)
Lee Roberts (Fermilab E989 experiment)
Thomas Teubner
Hartmut Wittig

White Paper (2020): $(g-2)_\mu$, experiment vs SM

White Paper:
T. Aoyama et al. Phys. Rep. 887 (2020) = WP(20)

Muon $g-2$ Theory Initiative
Workshops:

- 1st plenary meeting, Q-Center (Fermilab), 3-6 June 2017
- HVP WG workshop, KEK (Japan), 12-14 February 2018
- HLbL WG workshop, U. of Connecticut, 12-14 March 2018
- 2nd plenary meeting, Mainz, 18-22 June 2018
- 3rd plenary meeting, Seattle, 9-13 September 2019
- Lattice HVP workshop, virtual, 16-20 November 2020
- 4th plenary meeting, KEK (virtual), 28 June-02 July 2021
- 5th plenary meeting, Higgs Center Edinburgh, 5-9 Sept. 2022

White Paper executive summary (my own)

- QED and EW known and stable, negligible uncertainties
- HVP dispersive: consensus number, conservative uncertainty (KNT19, DHMZ19, CHS19, HHK19)
- HVP lattice: consensus number, $\Delta a_\mu^{\rm HVP,latt} \sim 5\,\Delta a_\mu^{\rm HVP,disp}$
  (Fermilab-HPQCD-MILC18,20, BMW18, RBC/UKQCD18, ETM19,SK19, Mainz19, ABTGJP20)
- HVP BMW20: central value $\to$ discrepancy $< 2\sigma$;
  $\Delta a_\mu^{\rm HVP,BMW} \sim \Delta a_\mu^{\rm HVP,disp}$ published 04/21 $\to$ not in WP
- HLbL dispersive: consensus number, w/ recent improvements $\Rightarrow$ $\Delta a_\mu^{\rm HLbL} \sim 0.5\,\Delta a_\mu^{\rm HVP}$
- HLbL lattice: single calculation, agrees with dispersive ($\Delta a_\mu^{\rm HLbL,latt} \sim 2\,\Delta a_\mu^{\rm HLbL,disp}$) $\to$ final average (RBC/UKQCD20)

Theory uncertainty comes from hadronic physics

- Hadronic contributions responsible for most of the theory uncertainty
- Hadronic vacuum polarization (HVP) is $\mathcal{O}(\alpha^2)$, dominates the total uncertainty, despite being known to $< 1\%$

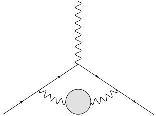

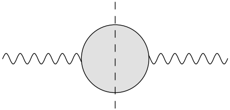

  - unitarity and analyticity $\Rightarrow$ dispersive approach
  - $\Rightarrow$ direct relation to experiment: $\sigma_{\rm tot}(e^+e^- \to \text{hadrons})$
  - e^+e^- Exps: BaBar, Belle, BESIII, CMD2/3, KLOE2, SND
  - alternative approach: lattice, becoming competitive

(BMW, ETMC, Fermilab, HPQCD, Mainz, MILC, RBC/UKQCD)

Theory uncertainty comes from hadronic physics

- Hadronic contributions responsible for most of the theory uncertainty
- Hadronic vacuum polarization (HVP) is $\mathcal{O}(\alpha^2)$, dominates the total uncertainty, despite being known to $< 1\%$
- Hadronic light-by-light (HLbL) is $\mathcal{O}(\alpha^3)$, known to $\sim 20\%$, second largest uncertainty (now subdominant)

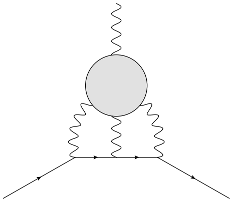

- earlier: model-based—uncertainties difficult to quantify
- recently: dispersive approach $\Rightarrow$ data-driven, systematic treatment
- lattice QCD is becoming competitive

(Mainz, RBC/UKQCD)

Outline

Introduction: $(g-2)_\mu$ in the Standard Model

Hadronic Vacuum Polarization contribution to $(g-2)_\mu$
- Data-driven approach
- Lattice approach: BMW result and its consequences

Hadronic light-by-light contribution to $(g-2)_\mu$
- Dispersive approach to the hadronic light-by-light tensor
- Short-distance constraints and axial vectors

Conclusions and Outlook

HVP contribution: Master Formula

Unitarity relation: simple, same for all intermediate states

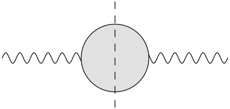

$$\mathrm{Im}\bar{\Pi}(q^2) \propto \sigma(e^+e^- \to \text{hadrons}) = \sigma(e^+e^- \to \mu^+\mu^-)R(q^2)$$

Analyticity $\left[\bar{\Pi}(q^2) = \frac{q^2}{\pi}\int ds \frac{\mathrm{Im}\bar{\Pi}(s)}{s(s-q^2)}\right] \Rightarrow$ Master formula for HVP

Bouchiat, Michel (61)

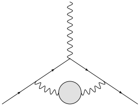

$$\Leftrightarrow \qquad a_\mu^{\mathrm{hvp}} = \frac{\alpha^2}{3\pi^2}\int_{s_{th}}^\infty \frac{ds}{s} K(s)R(s)$$

$K(s)$ known, depends on m_μ and $K(s) \sim \frac{1}{s}$ for large s

Comparison between DHMZ19 and KNT19

	DHMZ19	KNT19	Difference
$\pi^+\pi^-$	507.85(0.83)(3.23)(0.55)	504.23(1.90)	3.62
$\pi^+\pi^-\pi^0$	46.21(0.40)(1.10)(0.86)	46.63(94)	-0.42
$\pi^+\pi^-\pi^+\pi^-$	13.68(0.03)(0.27)(0.14)	13.99(19)	-0.31
$\pi^+\pi^-\pi^0\pi^0$	18.03(0.06)(0.48)(0.26)	18.15(74)	-0.12
K^+K^-	23.08(0.20)(0.33)(0.21)	23.00(22)	0.08
K_SK_L	12.82(0.06)(0.18)(0.15)	13.04(19)	-0.22
$\pi^0\gamma$	4.41(0.06)(0.04)(0.07)	4.58(10)	-0.17
Sum of the above	626.08(0.95)(3.48)(1.47)	623.62(2.27)	2.46
$[1.8, 3.7]$ GeV (without $c\bar{c}$)	33.45(71)	34.45(56)	-1.00
J/ψ, $\psi(2S)$	7.76(12)	7.84(19)	-0.08
$[3.7, \infty)$ GeV	17.15(31)	16.95(19)	0.20
Total $a_\mu^{\text{HVP, LO}}$	$694.0(1.0)(3.5)(1.6)(0.1)_\psi(0.7)_{\text{DV+QCD}}$	692.8(2.4)	1.2

2π: comparison with the dispersive approach

The 2π channel can itself be described dispersively $\Rightarrow$ more constrained theoretically Ananthanarayan, Caprini, Das (19), GC, Hoferichter, Stoffer (18)

Energy range	ACD18	CHS18	DHMZ19	KNT19
$\leq$ 0.6 GeV		110.1(9)	110.4(4)(5)	108.7(9)
$\leq$ 0.7 GeV		214.8(1.7)	214.7(0.8)(1.1)	213.1(1.2)
$\leq$ 0.8 GeV		413.2(2.3)	414.4(1.5)(2.3)	412.0(1.7)
$\leq$ 0.9 GeV		479.8(2.6)	481.9(1.8)(2.9)	478.5(1.8)
$\leq$ 1.0 GeV		495.0(2.6)	497.4(1.8)(3.1)	493.8(1.9)
[0.6, 0.7] GeV		104.7(7)	104.2(5)(5)	104.4(5)
[0.7, 0.8] GeV		198.3(9)	199.8(0.9)(1.2)	198.9(7)
[0.8, 0.9] GeV		66.6(4)	67.5(4)(6)	66.6(3)
[0.9, 1.0] GeV		15.3(1)	15.5(1)(2)	15.3(1)
$\leq$ 0.63 GeV	132.9(8)	132.8(1.1)	132.9(5)(6)	131.2(1.0)
[0.6, 0.9] GeV		369.6(1.7)	371.5(1.5)(2.3)	369.8(1.3)
$\left[\sqrt{0.1}, \sqrt{0.95}\right]$ GeV		490.7(2.6)	493.1(1.8)(3.1)	489.5(1.9)

WP(20)

Combination method and final result

Complete analyses DHMZ19 and KNT19, as well as CHS19 (2π) and HHK19 (3π), have been so combined:

- central values are obtained by simple averages (for each channel and mass range)
- the largest experimental and systematic uncertainty of DHMZ and KNT is taken
- $1/2$ difference DHMZ$-$KNT (or BABAR$-$KLOE in the 2π channel, if larger) is added to the uncertainty

Final result:

$$
\begin{aligned}
a_\mu^{\text{HVP, LO}} &= 693.1(2.8)_{\text{exp}}(2.8)_{\text{sys}}(0.7)_{\text{DV+QCD}} \times 10^{-10} \\
&= 693.1(4.0) \times 10^{-10}
\end{aligned}
$$

WP(20)

The BMW result

Borsanyi et al. Nature 2021

State-of-the-art lattice calculation of $a_\mu^{\text{HVP, LO}}$ based on

- current-current correlator, summed over all distances, integrated in time with appropriate kernel function (TMR)
- using staggered fermions on an $L \sim 6$ fm lattice ($L \sim 11$fm used for finite volume corrections)
- at (and around) physical quark masses
- including isospin-breaking effects

$\longrightarrow$ talk by T. Blum

The BMW result

Borsanyi et al. Nature 2021

Isospin-symmetric

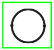

Connected light

$633.7(2.1)_{stat}(4.2)_{syst}$

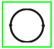

Connected strange

$53.393(89)_{stat}(68)_{syst}$

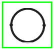

Connected charm

$14.6(0)_{stat}(1)_{syst}$

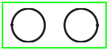

Disconnected

$-13.36(1.18)_{stat}(1.36)_{syst}$

QED isospin breaking: valence

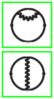

Connected $-1.23(40)_{stat}(31)_{syst}$

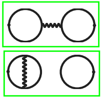

Disconnected $-0.55(15)_{stat}(10)_{syst}$

Strong–isospin breaking

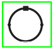

Connected

$6.60(63)_{stat}(53)_{syst}$

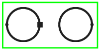

Disconnected

$-4.67(54)_{stat}(69)_{syst}$

QED isospin breaking: sea

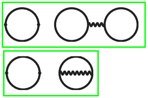

Connected $0.37(21)_{stat}(24)_{syst}$

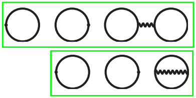

Disconnected $-0.040(33)_{stat}(21)_{syst}$

Other

Bottom; higher-order; perturbative

$0.11(4)_{tot}$

QED isospin breaking: mixed

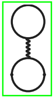

Connected $-0.0093(86)_{stat}(95)_{syst}$

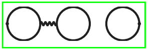

Disconnected $0.011(24)_{stat}(14)_{syst}$

Finite-size effects

Isospin-symmetric

$18.7(2.5)_{tot}$

Isospin-breaking

$0.0(0.1)_{tot}$

$$a_\mu^{\text{LO-HVP}}\ (\times 10^{10}) = 707.5(2.3)_{stat}(5.0)_{syst}(5.5)_{tot}$$

The BMW result

Borsanyi et al. Nature 2021

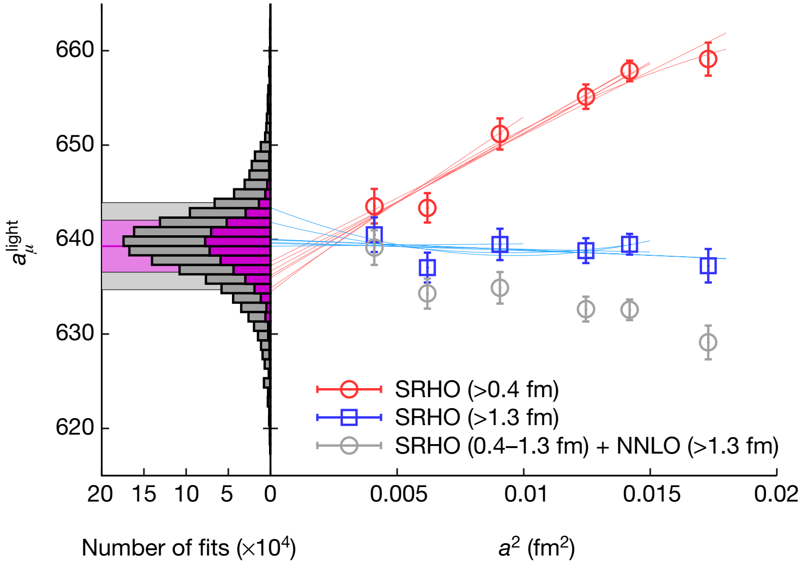

The BMW result

Borsanyi et al. Nature 2021

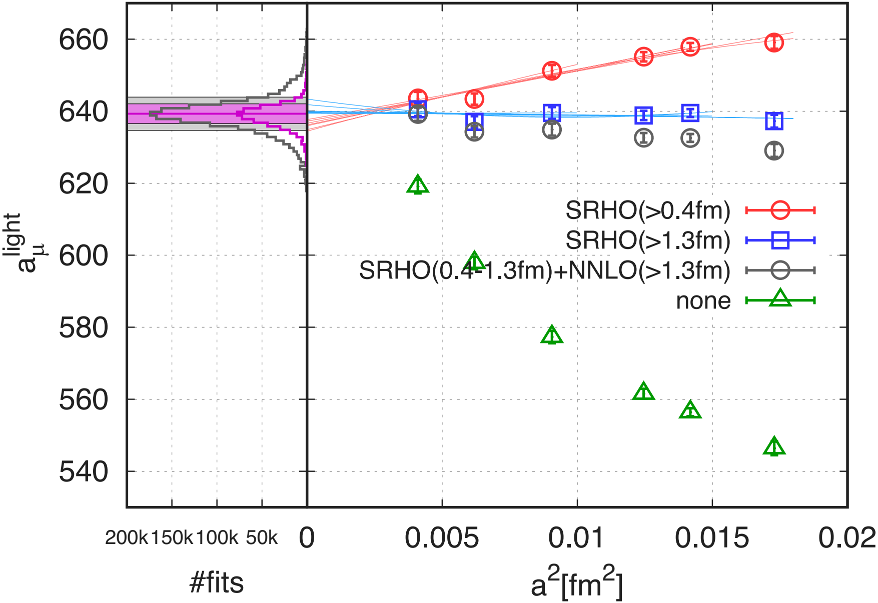

The BMW result

Borsanyi et al. Nature 2021

Article

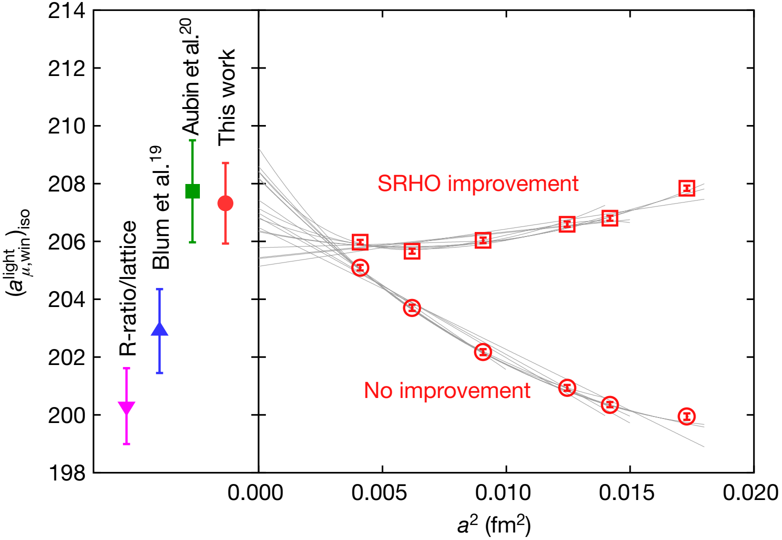

The BMW result

Borsanyi et al. Nature 2021

Weight functions for window quantities

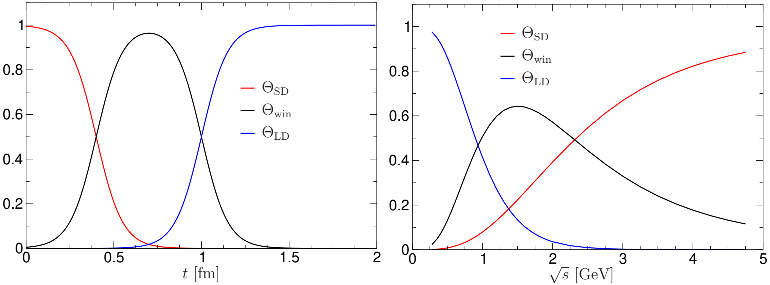

The BMW result

Borsanyi et al. Nature 2021

Summary: *ud* contribution

f	$a_\mu^{SD}(f)\cdot 10^{10}$	$a_\mu^{W}(f)\cdot 10^{10}$	$a_\mu^{LD}(f)\cdot 10^{10}$
ud	48.2 (0.8)	202.2 (2.6)	382.5 (11.7)

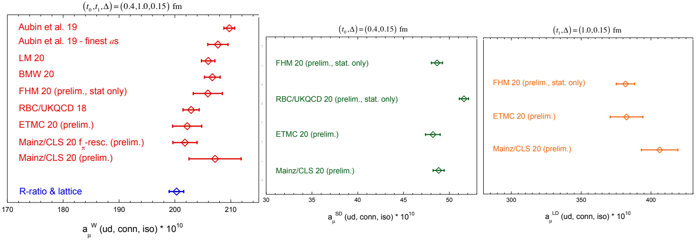

13

D. Giusti, talk at Lattice 2021

Present status of the window quantities

Several lattice calculations now confirm BMW's result

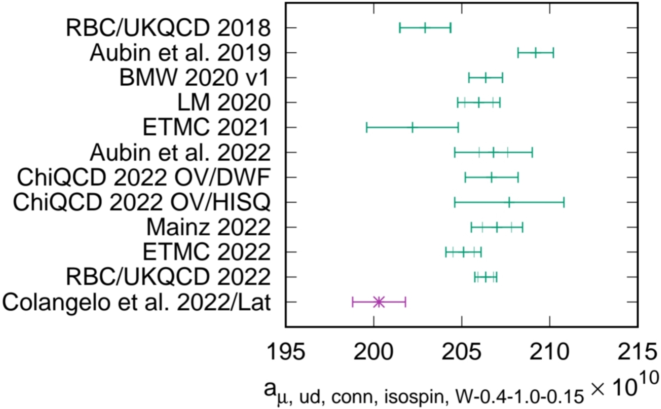

R-ratio: GC, El-Khadra, Hoferichter, Keshavarzi, Lehner, Stoffer, Teubner (22)

Plot by C. Lehner, Edinburgh 2022

Individual-channel contributions to $a_\mu^{\rm win}$

Channel	total	window
$\pi^+\pi^-$	504.23(1.90)	144.08(49)
$\pi^+\pi^-\pi^0$	46.63(94)	18.63(35)
$\pi^+\pi^-\pi^+\pi^-$	13.99(19)	8.88(12)
$\pi^+\pi^-\pi^0\pi^0$	18.15(74)	11.20(46)
K^+K^-	23.00(22)	12.29(12)
K_SK_L	13.04(19)	6.81(10)
$\pi^0\gamma$	4.58(10)	1.58(4)
Sum of the above	623.62(2.27)	203.47(78)
$[1.8, 3.7]$ GeV (without $c\bar{c}$)	34.45(56)	15.93(26)
$J/\psi, \psi(2S)$	7.84(19)	2.27(6)
$[3.7, \infty)$ GeV	16.95(19)	1.56(2)
WP(20) / GC, El-Khadra *et al.* (22)	693.1(4.0)	229.4(1.4)
BMWc	707.5(5.5)	236.7(1.4)
Mainz/CLS		237.3(1.5)
ETMc		235.0(1.1)
RBC/UKQCD		235.6(0.8)

Numbers for the channels refer to KNT19 — thanks to Alex Keshavarzi for providing them

$$\Delta a_\mu^{\text{HVP, LO}} = 14.4(6.8)\,(2.1\sigma), \qquad \Delta a_\mu^{\rm win} \sim 6.5(1.5)\,(\sim 4.3\sigma)$$

Consequences of the BMW result

A shift in the value of $a_\mu^{\text{HVP, LO}}$ would have consequences:

- $\Delta a_\mu^{\text{HVP, LO}} \quad \Leftrightarrow \quad \Delta\sigma(e^+e^- \to \text{hadrons})$
- $\Delta\alpha_{\text{had}}(M_Z^2)$ is determined by an integral of the same $\sigma(e^+e^- \to \text{hadrons})$ (more weight at high energy)
- changing $a_\mu^{\text{HVP, LO}}$ necessarily implies a shift in $\Delta\alpha_{\text{had}}(M_Z^2)$: size depends on the energy range of $\Delta\sigma(e^+e^- \to \text{hadrons})$
- a shift in $\Delta\alpha_{\text{had}}(M_Z^2)$ has an impact on the EW-fit
- to save the EW-fit $\Delta\sigma(e^+e^- \to \text{hadrons})$ must occur below $\sim$ 1 (max 2) GeV

  Crivellin, Hoferichter, Manzari, Montull (20)/Keshavarzi, Marciano, Passera, Sirlin (20)/Malaescu, Schott (20)
- or the need for BSM physics would be moved elsewhere

$\sigma(e^+e^- \to \pi^+\pi^-)$ and $F_\pi^V(s)$

- Below $1-2$ GeV only one significant channel: $\pi^+\pi^-$
- Strongly constrained by analyticity and unitarity ($F_\pi^V(s)$)
- $F_\pi^V(s)$ parametrization which satisfies these
  $\Rightarrow$ small number of parameters GC, Hoferichter, Stoffer (18)
- $\Delta a_\mu^{\text{HVP, LO}} \quad \Leftrightarrow \quad$ shifts in these parameters
  analysis of the corresponding scenarios GC, Hoferichter, Stoffer (21)

Vector form factor of the pion

$$\langle \pi^i(p')|V_\mu^k(0)|\pi^l(p)\rangle = i\epsilon^{ikl}(p'+p)_\mu F_\pi^V(s) \qquad s=(p'-p)^2$$

Analyticity:

$$e^{-i\delta(s)}F_\pi^V(s) \in \mathbb{R} \text{ for } s+i\varepsilon,\ 4M_\pi^2 \le s < \infty$$

Exact solution: Omnès (58)

$$F_\pi^V(s) = P(s)\Omega(s) = P(s)\exp\left\{\frac{s}{\pi}\int_{4M_\pi^2}^\infty \frac{ds'}{s'}\frac{\delta(s')}{s'-s}\right\} \quad ,$$

$P(s)$ a polynomial $\Leftrightarrow$ behaviour of $F_\pi^V(s)$ for $s \to \infty$ (or zeros)

- normalization fixed by gauge invariance:

$$F_\pi^V(0)=1 \quad \overset{\text{no zeros}}{\Longrightarrow} \quad P(s)=1$$

- $e^+e^- \to \pi^+\pi^-$ data $\Rightarrow$ free parameters in $\Omega(t)$

Omnès representation including isospin breaking

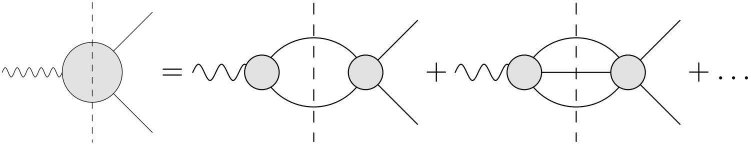

Omnès representation including isospin breaking

- Omnès representation

$$F_\pi^V(s) = \exp\left[\frac{s}{\pi}\int_{4M_\pi^2}^\infty ds' \frac{\delta(s')}{s'(s'-s)}\right] \equiv \Omega(s)$$

- Split elastic ($\leftrightarrow \pi\pi$ phase shift, δ_1^1) from inelastic phase

$$\delta = \delta_1^1 + \delta_{\rm in} \quad \Rightarrow \quad F_\pi^V(s) = \Omega_1^1(s)\Omega_{\rm in}(s)$$

Eidelman-Lukaszuk: unitarity bound on $\delta_{\rm in}$

$$\sin^2\delta_{\rm in} \leq \frac{1}{2}\left(1-\sqrt{1-r^2}\right),\ r = \frac{\sigma^{I=1}_{e^+e^-\to\neq 2\pi}}{\sigma_{e^+e^-\to 2\pi}} \Rightarrow s_{\rm in} = (M_\pi + M_\omega)^2$$

- $\rho-\omega$–mixing $\qquad F_V(s) = \Omega_{\pi\pi}(s)\cdot\Omega_{\rm in}(s)\cdot G_\omega(s)$

$$G_\omega(s) = 1 + \epsilon\frac{s}{s_\omega - s} \qquad \text{where} \qquad s_\omega = (M_\omega - i\Gamma_\omega/2)^2$$

Fit results

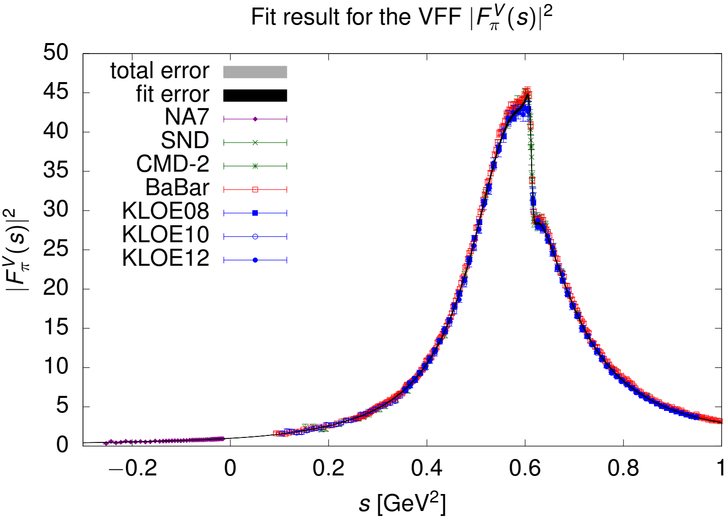

Fit result for the VFF $|F_\pi^V(s)|^2$
total error
fit error
NA7
SND
CMD-2
BaBar
KLOE08
KLOE10
KLOE12
$|F_\pi^V(s)|^2$
s [GeV^2]
50
45
40
35
30
25
20
15
10
5
0
−0.2
0
0.2
0.4
0.6
0.8
1

Fit results

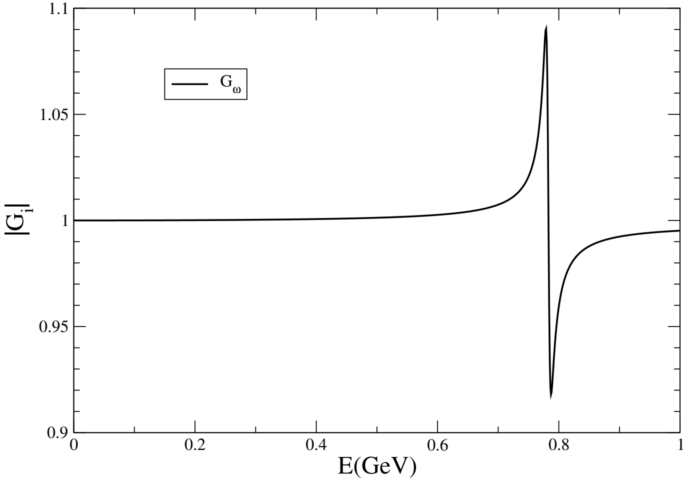

Fit results

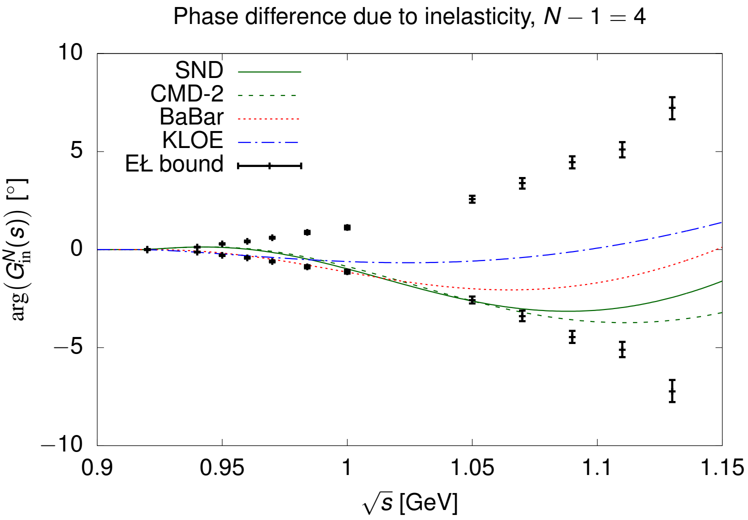

Phase difference due to inelasticity, $N-1=4$
SND
CMD-2
BaBar
KLOE
EŁ bound
$\arg(G_{in}^N(s))$ [°]
$\sqrt{s}$ [GeV]
10
5
0
−5
−10
0.9
0.95
1
1.05
1.1
1.15

Fit results

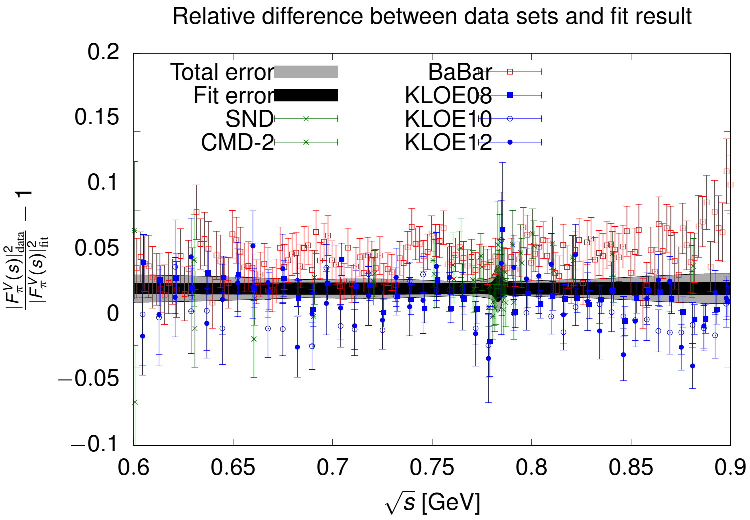

Relative difference between data sets and fit result
Total error
Fit error
SND
CMD-2
BaBar
KLOE08
KLOE10
KLOE12
$\frac{|F_\pi^V(s)|^2_{\text{data}}}{|F_\pi^V(s)|^2_{\text{fit}}} - 1$
$\sqrt{s}$ [GeV]
0.2
0.15
0.1
0.05
0
−0.05
−0.1
0.6
0.65
0.7
0.75
0.8
0.85
0.9

Change $\sigma(e^+e^- \to \pi^+\pi^-)|_{\sqrt{s}<1\text{GeV}}$ to agree w/ BMW

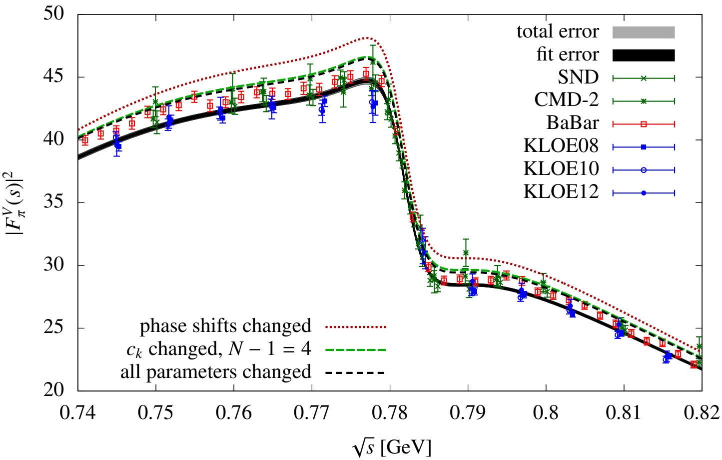

GC, Hoferichter, Stoffer (21)

Tension [BMW20 vs e^+e^- data] stronger for KLOE than for BABAR

Change $\sigma(e^+e^- \to \pi^+\pi^-)|_{\sqrt{s}<1\text{GeV}}$ to agree w/ BMW

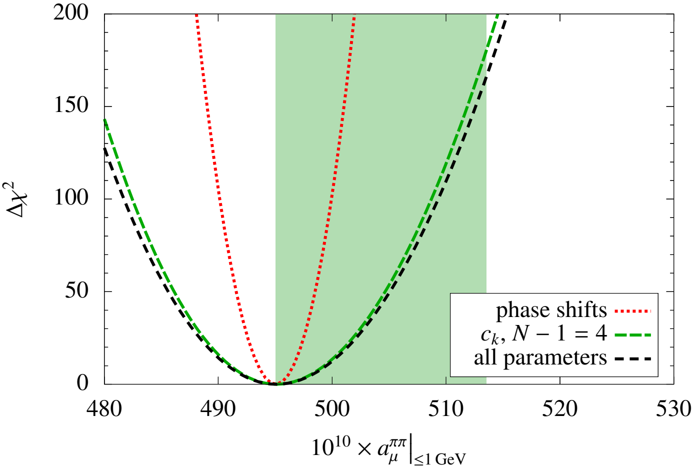

GC, Hoferichter, Stoffer (21)

Change $\sigma(e^+e^- \to \pi^+\pi^-)|_{\sqrt{s}<1\mathrm{GeV}}$ to agree w/ BMW

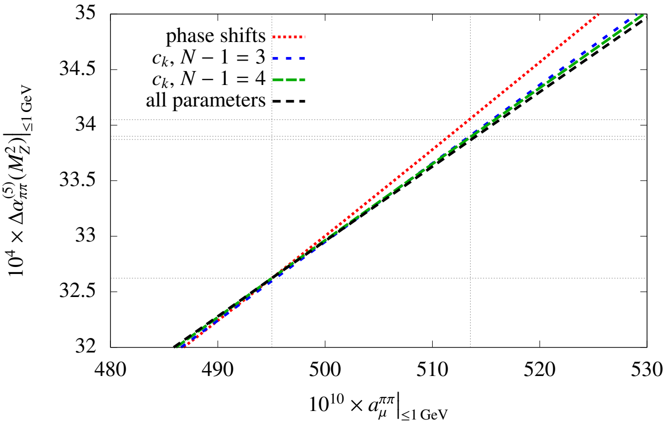

GC, Hoferichter, Stoffer (21)

$$10^4\Delta\alpha^{(5)}_{\mathrm{had}}(M_Z^2) = \begin{cases} 272.2(4.1) & \text{EW fit} \\ 276.1(1.1) & \sigma_{\mathrm{had}}(s) \end{cases}$$

Change $\sigma(e^+e^- \to \pi^+\pi^-)|_{\sqrt{s}<1\mathrm{GeV}}$ to agree w/ BMW

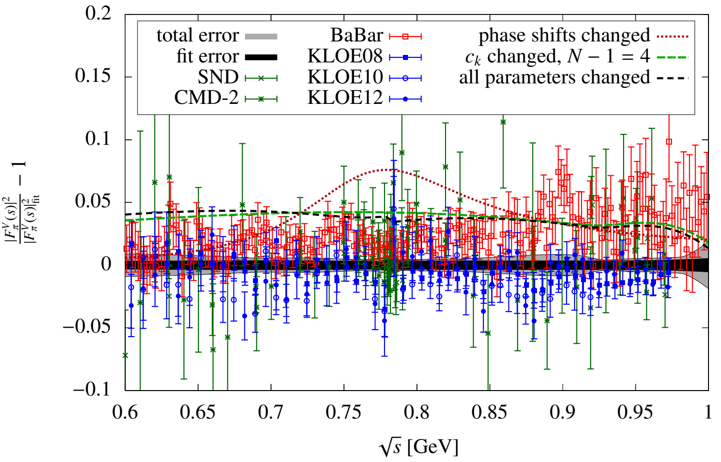

GC, Hoferichter, Stoffer (21)

Change $\sigma(e^+e^- \to \pi^+\pi^-)|_{\sqrt{s}<1\text{GeV}}$ to agree w/ BMW

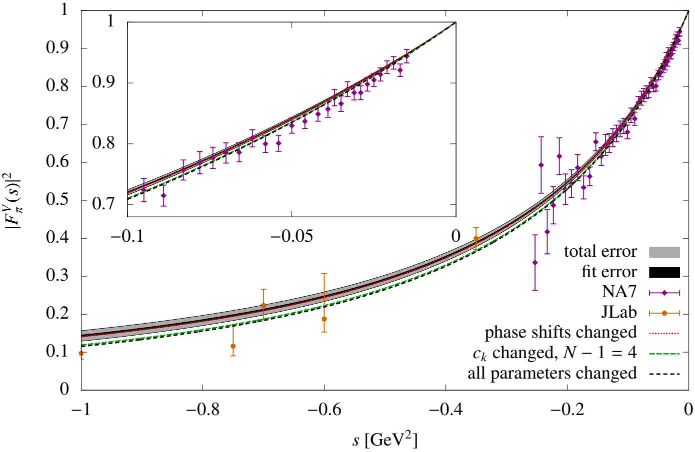

GC, Hoferichter, Stoffer (21)

How does the change in $(2\pi, < 1\,\mathrm{GeV})$ affect a_μ^{win}?

Channel	total	window
$\pi^+\pi^-$	504.23(1.90)	144.08(49)
$\pi^+\pi^-\pi^0$	46.63(94)	18.63(35)
$\pi^+\pi^-\pi^+\pi^-$	13.99(19)	8.88(12)
$\pi^+\pi^-\pi^0\pi^0$	18.15(74)	11.20(46)
K^+K^-	23.00(22)	12.29(12)
K_SK_L	13.04(19)	6.81(10)
$\pi^0\gamma$	4.58(10)	1.58(4)
Sum of the above	623.62(2.27)	203.47(78)
$[1.8, 3.7]$ GeV (without $c\bar{c}$)	34.45(56)	15.93(26)
J/ψ, $\psi(2S)$	7.84(19)	2.27(6)
$[3.7, \infty)$ GeV	16.95(19)	1.56(2)
WP(20) / GC, El-Khadra *et al.* (22)	693.1(4.0)	229.4(1.4)
BMWc	707.5(5.5)	236.7(1.4)
Mainz/CLS		237.3(1.5)
ETMc		235.0(1.1)
RBC/UKQCD		235.6(0.8)

Numbers for the channels refer to KNT19 — thanks to Alex Keshavarzi for providing them

$$\Delta a_\mu^{\text{HVP, LO}} = 14.4(6.8)\,(2.1\sigma), \qquad \Delta a_\mu^{\mathrm{win}} \sim 6.5(1.5)\,(\sim 4.3\sigma)$$

How does the change in $(2\pi, < 1\mathrm{GeV})$ affect a_μ^{win}?

Channel	total	window
$\pi^+\pi^-$	518.6	148
$\pi^+\pi^-\pi^0$	46.63(94)	18.63(35)
$\pi^+\pi^-\pi^+\pi^-$	13.99(19)	8.88(12)
$\pi^+\pi^-\pi^0\pi^0$	18.15(74)	11.20(46)
K^+K^-	23.00(22)	12.29(12)
K_SK_L	13.04(19)	6.81(10)
$\pi^0\gamma$	4.58(10)	1.58(4)
Sum of the above	638.0	207.5
$[1.8, 3.7]$ GeV (without $c\bar{c}$)	34.45(56)	15.93(26)
J/ψ, $\psi(2S)$	7.84(19)	2.27(6)
$[3.7, \infty)$ GeV	16.95(19)	1.56(2)
WP(20) / GC, El-Khadra *et al.* (22)	707.5	233.4
BMWc	707.5(5.5)	236.7(1.4)
Mainz/CLS		237.3(1.5)
ETMc		235.0(1.1)
RBC/UKQCD		235.6(0.8)

Numbers for the channels refer to KNT19 — thanks to Alex Keshavarzi for providing them

$$\Delta a_\mu^{\text{HVP, LO}} = 0, \qquad \Delta a_\mu^{\mathrm{win}} \sim 2.5$$

What does this tell us about $\sqrt{s}$-range of $\Delta\sigma(e^+e^-)$?

- $\Delta\sigma(e^+e^-)$ all < 1 GeV does not allow one to satisfy simultaneously $\Delta a_\mu^{\text{HVP, LO}} = 0$ and $\Delta a_\mu^{\text{win}} = 0$
- $\Delta\sigma(e^+e^-)$ must happen < 2 GeV (EWFit)

Weight function $\in (0.5, 0.65)$

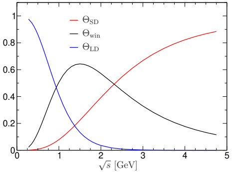

- assume reasonable shape of $\Delta\sigma(e^+e^-)$ (no negative shifts)

$\Rightarrow$ at least 40% of $\Delta a_\mu^{\text{HVP, LO}} = 14.4$ from above 1 GeV

What does this tell us about $\sqrt{s}$-range of $\Delta\sigma(e^+e^-)$?

Channel	total	window
$\pi^+\pi^-$	504.23(1.90)	144.08(49)
$\pi^+\pi^-\pi^0$	46.63(94)	18.63(35)
$\pi^+\pi^-\pi^+\pi^-$	13.99(19)	8.88(12)
$\pi^+\pi^-\pi^0\pi^0$	18.15(74)	11.20(46)
K^+K^-	23.00(22)	12.29(12)
K_SK_L	13.04(19)	6.81(10)
$\pi^0\gamma$	4.58(10)	1.58(4)
Sum of the above	623.62(2.27)	203.47(78)
$[1.8, 3.7]$ GeV (without $c\bar{c}$)	34.45(56)	15.93(26)
J/ψ, $\psi(2S)$	7.84(19)	2.27(6)
$[3.7, \infty)$ GeV	16.95(19)	1.56(2)
WP(20) / GC, El-Khadra *et al.* (22)	693.1(4.0)	229.4(1.4)
BMWc	707.5(5.5)	236.7(1.4)
Mainz/CLS		237.3(1.5)
ETMc		235.0(1.1)
RBC/UKQCD		235.6(0.8)

Numbers for the channels refer to KNT19 — thanks to Alex Keshavarzi for providing them

Fermilab/HPQCD/MILC result $\longrightarrow$ talk by S. Gottlieb

Outline

Introduction: $(g-2)_\mu$ in the Standard Model

Hadronic Vacuum Polarization contribution to $(g-2)_\mu$
- Data-driven approach
- Lattice approach: BMW result and its consequences

Hadronic light-by-light contribution to $(g-2)_\mu$
- Dispersive approach to the hadronic light-by-light tensor
- Short-distance constraints and axial vectors

Conclusions and Outlook

Calculating the HLbL contribution

The HLbL contribution is a very complex quantity

- 4-point function of em currents in QCD

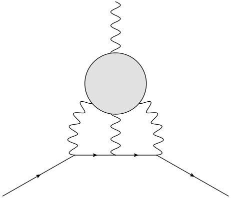

- early on, it has been calculated with models

  Hayakawa-Kinoshita-Sanda/Bijnens-Pallante-Prades (96), Knecht, Nyffeler (02), Melnikov, Vainshtein (04)

- a data-driven approach, like for HVP, has only recently been developed and used

  GC, Hoferichter, Procura, Stoffer=CHPS (14,15,17), Hoferichter, Hoid, Kubis, Leupold, Schneider (18)

- lattice QCD is becoming competitive RBC/UKQCD (20), Mainz (21)

Different model-based evaluations of HLbL

Jegerlehner-Nyffeler 2009

Contribution	BPaP(96)	HKS(96)	KnN(02)	MV(04)	BP(07)	PdRV(09)	N/JN(09)
π^0, η, η'	85±13	82.7±6.4	83±12	114±10	–	114±13	99±16
π, K loops	−19±13	−4.5±8.1	–	–	–	−19±19	−19±13
" " + subl. in N_c	–	–	–	0±10	–	–	–
axial vectors	2.5±1.0	1.7±1.7	–	22± 5	–	15±10	22± 5
scalars	−6.8±2.0	–	–	–	–	−7± 7	−7± 2
quark loops	21± 3	9.7±11.1	–	–	–	2.3	21± 3
total	83±32	89.6±15.4	80±40	136±25	110±40	105±26	116±39

Legenda: B=Bijnens Pa=Pallante P=Prades H=Hayakawa K=Kinoshita S=Sanda Kn=Knecht N=Nyffeler M=Melnikhov V=Vainshtein dR=de Rafael J=Jegerlehner

- large uncertainties (and differences among calculations) in individual contributions
- pseudoscalar pole contributions most important
- second most important: pion loop, *i.e.* two-pion cuts (*Ks are subdominant*)
- heavier single-particle poles decreasingly important

Advantages of the dispersive approach

- model independent
- unambiguous definition of the various contributions
- makes a data-driven evaluation possible
  (in principle)
- if data not available: use theoretical calculations of subamplitudes, short-distance constraints etc.
- First attempts: GC, Hoferichter, Procura, Stoffer (14), Pauk, Vanderhaeghen (14)

  [Schwinger sum rule: Hagelstein, Pascalutsa (17)]

HLbL contribution: Master Formula

$$a_\mu^{\mathrm{HLbL}} = \frac{2\alpha^3}{48\pi^2}\int_0^\infty dQ_1 \int_0^\infty dQ_2 \int_{-1}^{1} d\tau \sqrt{1-\tau^2}\sum_{i=1}^{12} T_i(Q_1,Q_2,\tau)\bar{\Pi}_i(Q_1,Q_2,\tau)$$

Q_i^μ are the Wick-rotated four-momenta and τ the four-dimensional angle between Euclidean momenta:

$$Q_1 \cdot Q_2 = |Q_1||Q_2|\tau$$

The integration variables $Q_1 := |Q_1|$, $Q_2 := |Q_2|$.

GC, Hoferichter, Procura, Stoffer (15)

- T_i: known kernel functions
- $\bar{\Pi}_i$ are amenable to a dispersive treatment: imaginary parts are related to measurable subprocesses

Improvements obtained with the dispersive approach

Contribution	PdRV(09) *Glasgow consensus*	N/JN(09)	J(17)	WP(20)
π^0, η, η'-poles	114(13)	99(16)	95.45(12.40)	93.8(4.0)
π, K-loops/boxes	−19(19)	−19(13)	−20(5)	−16.4(2)
S-wave $\pi\pi$ rescattering	−7(7)	−7(2)	−5.98(1.20)	−8(1)
subtotal	88(24)	73(21)	69.5(13.4)	69.4(4.1)
scalars	–	–	–	− 1(3) (scalars and tensors together)
tensors	–	–	1.1(1)	
axial vectors	15(10)	22(5)	7.55(2.71)	6(6)
u, d, s-loops / short-distance	–	21(3)	20(4)	15(10)
c-loop	2.3	–	2.3(2)	3(1)
total	105(26)	116(39)	100.4(28.2)	92(19)

- significant reduction of uncertainties in the first three rows
  CHPS (17), Masjuan, Sánchez-Puertas (17) Hoferichter, Hoid et al. (18), Gerardin, Meyer, Nyffeler (19)
- 1 − 2 GeV resonances affected by basis ambiguity and large uncertainties Danilkin, Hoferichter, Stoffer (21)]
- asymptotic region recently addressed, Melnikov, Vainshtein (04), Nyffeler (09), WP still work in progress Bijnens et al. (20,21), Cappiello et al. (20), Leutgeb, Rebhan (19,21)

Situation for HLbL

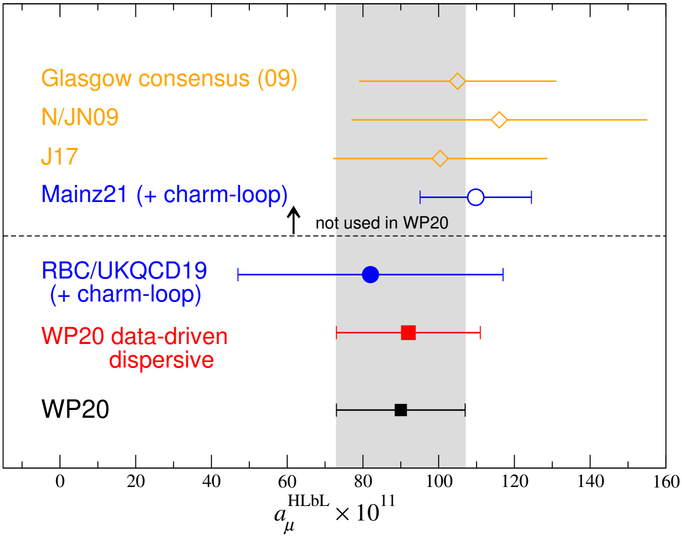

Longitudinal SDCs: a few definitions

The longitudinal SDC only concerns one function: Π_1

Split π^0-pole from the rest in general kinematics ($q_4^2 = 0,\ q_4^\mu \neq 0$):

$$\Pi_1(s,t,u) = \frac{F_{\pi\gamma^*\gamma^*}(q_1^2,q_2^2)F_{\pi\gamma\gamma^*}(q_3^2)}{s-M_\pi^2} + G(s,t,u)$$

For $g-2$ kinematics ($q_4^\mu \to 0, \Rightarrow\ s = q_3^2,\ t = q_2^2,\ u = q_1^2$):

$$\begin{aligned}\bar\Pi_1(q_3^2,q_2^2,q_1^2) &= \frac{F_{\pi\gamma^*\gamma^*}(q_1^2,q_2^2)F_{\pi\gamma\gamma^*}(q_3^2)}{q_3^2-M_\pi^2} + G(q_3^2,q_2^2,q_1^2)\\ &= \frac{F_{\pi\gamma^*\gamma^*}(q_1^2,q_2^2)}{q_3^2-M_\pi^2}\left[F_{\pi\gamma\gamma^*}(M_\pi^2) + \bar F_{\pi\gamma\gamma^*}(q_3^2)\right] + G(q_3^2,q_2^2,q_1^2)\end{aligned}$$

with $\bar F_{\pi\gamma\gamma^*}(q_3^2) \equiv F_{\pi\gamma\gamma^*}(q_3^2) - F_{\pi\gamma\gamma^*}(M_\pi^2)$

Longitudinal SDCs: a few definitions

The longitudinal SDC only concerns one function: Π_1

Split π^0-pole from the rest in general kinematics ($q_4^2 = 0,\ q_4^\mu \neq 0$):

$$\Pi_1(s,t,u) = \frac{F_{\pi\gamma^*\gamma^*}(q_1^2,q_2^2)F_{\pi\gamma\gamma^*}(q_3^2)}{s-M_\pi^2} + G(s,t,u)$$

For $g-2$ kinematics ($q_4^\mu \to 0, \Rightarrow\ s = q_3^2,\ t = q_2^2,\ u = q_1^2$):

$$\bar{\Pi}_1(q_3^2,q_2^2,q_1^2) = \frac{F_{\pi\gamma^*\gamma^*}(q_1^2,q_2^2)F_{\pi\gamma\gamma^*}(q_3^2)}{q_3^2-M_\pi^2} + G(q_3^2,q_2^2,q_1^2)$$

$$= \frac{F_{\pi\gamma^*\gamma^*}(q_1^2,q_2^2)}{q_3^2-M_\pi^2}\left[F_{\pi\gamma\gamma^*}(M_\pi^2) + \bar{F}_{\pi\gamma\gamma^*}(q_3^2)\right] + G(q_3^2,q_2^2,q_1^2)$$

with $\bar{F}_{\pi\gamma\gamma^*}(q_3^2) \equiv F_{\pi\gamma\gamma^*}(q_3^2) - F_{\pi\gamma\gamma^*}(M_\pi^2)$

The longitudinal SDCs

Two different kinematic configurations for large q_i^2:

1. All momenta large — Melnikov-Vainshtein (04), Bijnens et al (19)

$$\bar{\Pi}_1(q^2,q^2,q^2) \overset{q^2\to\infty}{=} -\frac{4}{9\pi^2 q^4} + \mathcal{O}(q^{-6})$$

2. $q^2 \equiv q_1^2 \sim q_2^2 \gg q_3^2,\ q^2 \gg \Lambda^2_{\rm QCD}$: — Melnikov-Vainshtein (04)

$$\bar{\Pi}_1(q_3^2,q^2,q^2) \overset{q^2\to\infty}{=} -\frac{1}{9\pi^2 q^2} w_L(q_3^2) + \mathcal{O}(q^{-4})$$

with $w_L(q_3^2)$ the longitudinal amplitude in $\langle VVA\rangle$, *the anomaly*

The longitudinal SDCs

Two different kinematic configurations for large q_i^2:

1. All momenta large — Melnikov-Vainshtein (04), Bijnens et al (19)

$$\bar{\Pi}_1(q^2,q^2,q^2) \overset{q^2\to\infty}{=} -\frac{4}{9\pi^2 q^4} + \mathcal{O}(q^{-6})$$

2. $q^2 \equiv q_1^2 \sim q_2^2 \gg q_3^2,\ q^2 \gg \Lambda_{\rm QCD}^2$: — Melnikov-Vainshtein (04)

$$\bar{\Pi}_1(q_3^2,q^2,q^2) \overset{q^2\to\infty}{=} -\frac{1}{9\pi^2 q^2}\frac{6}{q_3^2} + \mathcal{O}(q^{-4})$$

In the chiral (and large-N_c) limit $w_L(q_3^2)$ is known exactly

$$w_L(q_3^2) = \frac{6}{q_3^2} \ \Rightarrow\ G(q_3^2,q^2,q^2)\Big|_{m_q=0} \overset{q\to\infty}{=} \frac{2F_\pi}{3q^2}\frac{\bar{F}_{\pi\gamma\gamma^*}(q_3^2)}{q_3^2}\Big|_{m_q=0} + \mathcal{O}(q^{-4})$$

No individual dispersive contribution satisfies these constraints

The longitudinal SDCs

Two different kinematic configurations for large q_i^2:

1. All momenta large — Melnikov-Vainshtein (04), Bijnens et al (19)

$$\bar{\Pi}_1(q^2,q^2,q^2) \overset{q^2\to\infty}{=} -\frac{4}{9\pi^2 q^4} + \mathcal{O}(q^{-6})$$

2. $q^2 \equiv q_1^2 \sim q_2^2 \gg q_3^2,\ q^2 \gg \Lambda^2_{\mathrm{QCD}}$: — Melnikov-Vainshtein (04)

$$\bar{\Pi}_1(q_3^2,q^2,q^2) \overset{q^2\to\infty}{=} -\frac{1}{9\pi^2 q^2}\frac{6}{q_3^2} + \mathcal{O}(q^{-4})$$

In the chiral (and large-N_c) limit $w_L(q_3^2)$ is known exactly

$$w_L(q_3^2) = \frac{6}{q_3^2} \;\Rightarrow\; G(q_3^2,q^2,q^2)\Big|_{m_q=0} \overset{q\to\infty}{=} \frac{2F_\pi}{3q^2}\frac{\bar{F}_{\pi\gamma\gamma^*}(q_3^2)}{q_3^2}\Big|_{m_q=0} + \mathcal{O}(q^{-4})$$

The π-pole for $g-2$ kinematics does — Melnikov-Vainshtein (04)

Recent activity on SDCs (mainly post WP)

- calculation of (non-)perturbative corrections to the OPE

  Bijnens, Hermansson-Truedsson, Laub, Rodríguez-Sánchez (20,21)

- tower of excited pseudoscalars (Regge model)

  GC, Hagelstein, Hoferichter, Laub, Stoffer (19)

- tower of axial-vectors (holographic QCD model)

  Leutgeb, Rebhan (19), Cappiello, Catà, D'Ambrosio, Greynat, Iyer (20)

- solution based on interpolants

  Lüdtke, Procura (20)

- general considerations, comparison of model solutions

  Knecht (20), Masjuan, Roig, Sánchez-Puertas (20), GC, Hagelstein, Hoferichter, Laub, Stoffer (21)

Recent activity on SDCs (mainly post WP)

- calculation of (non-)perturbative corrections to the OPE

  Bijnens, Hermansson-Truedsson, Laub, Rodríguez-Sánchez (20,21)
- tower of excited pseudoscalars (Regge model)

  GC, Hagelstein, Hoferichter, Laub, Stoffer (19)
- tower of axial-vectors (holographic QCD model)

  Leutgeb, Rebhan (19), Cappiello, Catà, D'Ambrosio, Greynat, Iyer (20)
- solution based on interpolants

  Lüdtke, Procura (20)
- general considerations, comparison of model solutions

  Knecht (20), Masjuan, Roig, Sánchez-Puertas (20), GC, Hagelstein, Hoferichter, Laub, Stoffer (21)

Melnikov-Vainshtein and holographic QCD

- Melnikov-Vainshtein model: Melnikov-Vainshtein (04)

$$w_L^{\rm MV}(q_3^2) = \frac{6}{q_3^2 - M_\pi^2} + \mathcal{O}(M_\pi^2)$$

$$G^{\rm MV}(q_i^2) = -\frac{F_{\pi\gamma^*\gamma^*}(q_1^2, q_2^2)\bar{F}_{\pi\gamma\gamma^*}(q_3^2)}{q_3^2} + \mathcal{O}(M_\pi^2)$$

- hQCD (HW2) model: Leutgeb, Rebhan (19), Cappiello et al. (20)

$$w_L^{\rm HW2}(q_3^2) = \frac{6}{q_3^2 - M_\pi^2}\left[1 + \frac{M_\pi^2 \bar{F}_{\pi\gamma\gamma^*}(q_3^2)}{q_3^2 F_{\pi\gamma\gamma}}\right]$$

$$G^{\rm HW2}(q_i^2) = -\frac{F_{\pi\gamma^*\gamma^*}(q_1^2, q_2^2)\bar{F}_{\pi\gamma\gamma^*}(q_3^2)}{q_3^2} - \frac{F_{\pi\gamma\gamma}^2}{q_3^2}\Delta G(q_i^2)$$

Melnikov-Vainshtein and holographic QCD

- Melnikov-Vainshtein model: Melnikov-Vainshtein (04)

$$w_L^{\rm MV}(q_3^2) = \frac{6}{q_3^2 - M_\pi^2} + \mathcal{O}(M_\pi^2)$$

$$G^{\rm MV}(q_i^2) = -\frac{F_{\pi\gamma^*\gamma^*}(q_1^2, q_2^2)\bar{F}_{\pi\gamma\gamma^*}(q_3^2)}{q_3^2} + \mathcal{O}(M_\pi^2)$$

- hQCD (HW2) model: Leutgeb, Rebhan (19), Cappiello et al. (20)

$$w_L^{\rm HW2}(q_3^2) = \frac{6}{q_3^2 - M_\pi^2}\left[1 + \frac{M_\pi^2 \bar{F}_{\pi\gamma\gamma^*}(q_3^2)}{q_3^2 F_{\pi\gamma\gamma}}\right]$$

$$G^{\rm HW2}(q_i^2) = -\frac{F_{\pi\gamma^*\gamma^*}(q_1^2, q_2^2)\bar{F}_{\pi\gamma\gamma^*}(q_3^2)}{q_3^2} - \frac{F_{\pi\gamma\gamma}^2}{q_3^2}\Delta G(q_i^2)$$

$$\equiv \quad MV(q_i^2) \quad + \quad NF(q_i^2)$$

Numerical comparison for w_L

GC, Hagelstein, Hoferichter, Laub, Stoffer (21)

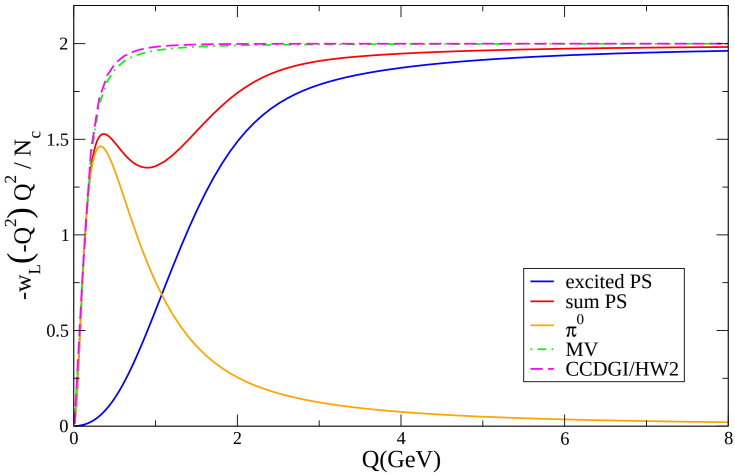

Numerical comparison for G

GC, Hagelstein, Hoferichter, Laub, Stoffer (21)

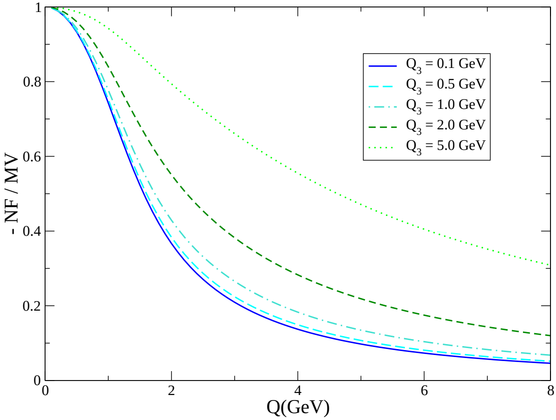

Numerical comparison for a_μ^{HLbL}

GC, Hagelstein, Hoferichter, Laub, Stoffer (21)

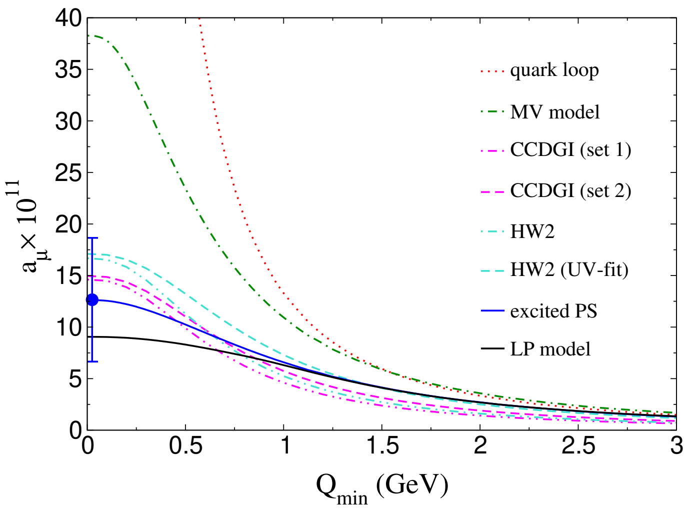

Comments on the contribution of axial vectors

- like all resonances besides pseudoscalars, axial vectors affected by basis ambiguity
- model calculations: large spread, $\Rightarrow$ axial-vector contributions might potentially be large (transverse SDC)

	$a_\mu^{\text{axials}}[a_1, f_1, f_1']$
– Melnikov, Vainshtein (04)	$22(5) \times 10^{-11}$
– Pauk, Vanderhaeghen (14)(only f_1, f_1')	$6.4(2.0) \times 10^{-11}$
– Jegerlehner (17)	$7.6(2.7) \times 10^{-11}$
– Roig, Sánchez-Puertas (20)	$0.8(^{+3.5}_{-0.8}) \times 10^{-11}$
– hQCD models (contribution only to T amplitudes)	
Leutgeb, Rebhan (19,21)	$\sim 17 \times 10^{-11}$
Cappiello et al. (20)	$\sim 14 \times 10^{-11}$

- model-independent treatment of axials particularly urgent

Recent work on axial-vector contributions

- New basis free of kinematic singularities for axials

  GC, Hagelstein, Hoferichter, Laub, Stoffer (21)

- Asymptotic behaviour of TFF of axial vectors

  Hoferichter, Stoffer (20)

- Analysis of phenomenological and asymptotic constraints on a VMD model for TFF of axial vectors

  Zanke, Hoferichter and Kubis (21)

- hQCD models with $m_q \neq 0$, including phenomenological and asymptotic constraints Leutgeb, Rebhan (21)

  Large contributions confirmed. hQCD models successful so far
  $\Rightarrow$ this needs to be understood

Outline

Introduction: $(g-2)_\mu$ in the Standard Model

Hadronic Vacuum Polarization contribution to $(g-2)_\mu$
- Data-driven approach
- Lattice approach: BMW result and its consequences

Hadronic light-by-light contribution to $(g-2)_\mu$
- Dispersive approach to the hadronic light-by-light tensor
- Short-distance constraints and axial vectors

Conclusions and Outlook

Conclusions

- The WP provides the current status of the SM evaluation of $(g-2)_\mu$: 4.2σ discrepancy with experiment (BNL+FNAL)

- Evaluation of the HVP contribution based on the dispersive approach: 0.6% error $\Rightarrow$ dominates the theory uncertainty

- Recent lattice calculation [BMW(20)] has reached a similar precision but differs from the dispersive one (=from e^+e^- data).
  If confirmed $\Rightarrow$ discrepancy with experiment $\searrow$ below 2σ

- For the intermediate window BMW has now been confirmed by several other lattice collaborations (Aubin et al., Mainz, ETMc, RBC/UKQCD)

- Evaluation of the HLbL contribution based on the dispersive approach: 20% accuracy. Two recent lattice calculations [RBC/UKQCD(20), Mainz(21)] agree with it

Outlook

- The Fermilab experiment aims to reduce the BNL uncertainty by a factor four $\Rightarrow$ potential 7σ discrepancy
- Improvements on the SM theory/data side:
  - HVP data-driven:
    Other e^+e^- experiments are available or forthcoming:
    SND, BaBar, Belle II, BESIII, CMD3 $\Rightarrow$ Error reduction
    MuonE will provide an alternative way to measure HVP
  - HVP lattice:
    calculations with precision $\sim$ BMW for $a_\mu^{\text{HVP, LO}}$ are awaited
    For a_μ^{win}, the difference to the data-driven evaluation is a puzzle and must be understood
  - HLbL data-driven: goal of $\sim$ 10% uncertainty within reach
  - HLbL lattice: RBC/UKQCD $\Rightarrow$ similar precision as Mainz.
    Good agreement with data-driven evaluation.

Future: Muon $g-2$/EDM experiment @ J-PARC

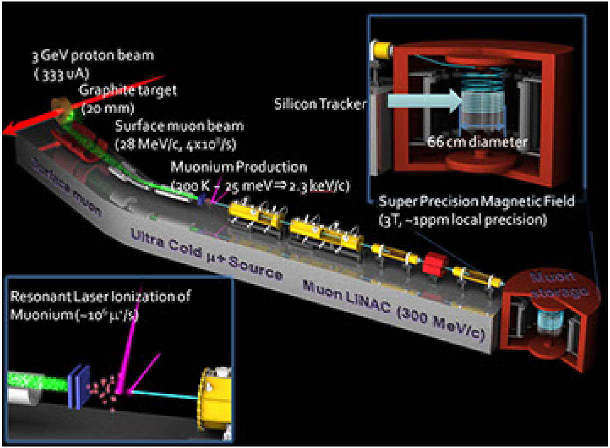

Credit: J-PARC